International Journal of Electrical and Computer Engineering (IJECE)
Vol. 10, No. 2, April 2020, pp. 1113~1121
ISSN: 2088-8708, DOI: 10.11591/ijece.v10i2.pp1113-1121

A solar fed BLDC motor drive for mixer grinder using a buck converter

Deekshitha S Nayak, R. Shivarudraswamy
Department of Electrical and Electronics Engineering, Manipal Institute of Technology, India

Article Info

Article history:

Received Jun 3, 2019
Revised Oct 11, 2019
Accepted Oct 20, 2019

Keywords:

BLDC
Hysteresis current control
MATLAB
Mixer grinder
Solar

ABSTRACT

In large and small scale applications, different kinds of variable speed driving systems can be found. For saving the energy consumption of these devices, eco-friendly electronics are used, which lead to the development of the Brushless DC motor (BLDC). Its higher power density, higher efficiency, higher torque at low speed, and low maintenance enhances the use of a BLDC motor. The existing mixer grinder consists of the universal motor, which operates in alternating current supply due to high starting torque characteristics and simple controlling of the speed. The absence of brushes and the reduction of noise in the BLDC extends its life and makes it ideal in a mixer grinder. A solar-powered BLDC motor drive for a mixer grinder is presented in this paper. A DC-DC buck converter is utilized to operate the PV (photovoltaic) array at its maximum power. The proposed hysteresis current control BLDC system has been developed in the MATLAB. The commercially available mixer grinder is presented along with the proposed simulated system for performance comparison. It can be concluded that at the no load condition, the efficiency of the experimental existing mixer grinder is 51.03% and simulated proposed system is 81.25% and at load condition, the efficiency of the experimental mixer grinder is 49.32% and simulated system is 79.85%.

Corresponding Author:

R. Shivarudraswamy,
Department of Electrical and Electronics Engineering,
Manipal Institute of Technology,
Manipal Academy of Higher Education, Manipal, Karnataka, India
Email: shivarudraswamy.r@manipal.edu

1. INTRODUCTION

In recent years, due to the varied climate conditions and energy security, solar generating arrangement has gained extensive attention [1, 2]. Solar energy is used in domestic appliances like the mixer grinder in remote regions where power transmission is impractical. In the commercially available mixer grinder, the universal motor is used [3, 4]. In addition to the low efficiency of a universal motor, it needs regular maintenance due to the commutators and brush arrangements [5]. The BLDC motor with an electronic commutator requires no maintenance and is highly efficient. In comparison with the universal motor, the BLDC motor has unity power factor and high power density [6, 7]. Figure 1 presents a diagram of the proposed BLDC motor drive used in the mixer grinder. The high efficiency of the BLDC motor decreases the size of the PV array and the installation cost. Its higher power factor reduces the capacity of the used voltage source inverter (VSI) [8]. A buck converter is placed between the solar array and the voltage source inverter (VSI). Additionally, the buck converter is operated by controlling the PV array through the Perturb and Observer MPPT algorithm technique [9-10]. The BLDC mixer grinder is fed by the VSI. The three current sensors and hall sensors are fed to a BLDC motor control. The BLDC motor control is the hysteresis current controller, and gate signals from the controller are fed to a VSI for controlling the speed of the motor.

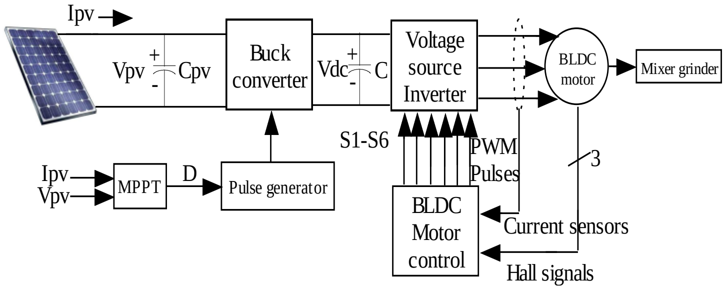

Figure 1. Schematic diagram of proposed mixer grinder

2. RESEARCH METHOD

The mathematical modelling of the BLDC motor and the proposed speed control by hysteresis current controller is explained below.

2.1. Modelling of the BLDC drive system

To run the motor at different speeds, the BLDC motor drive requires a speed controller for smooth control of the drive [11]. A closed loop speed controller of the BLDC motor drive is depicted in Figure 2. In the closed loop operation, the time reference speed can be varied for the drive to work at the desired speed. In the closed loop speed controller drive, the actual speed of the motor is fed back as input. By using the control systems, the speed can be varied as required. The actual speed is fed back as input and is measured with a reference speed values, which generates the error signals. This is fed to the PI controller, which controls the speed [12, 13]. The past and the present error gets nullifies by the PI controller. The speed fed to the PI controller generates reference torque values. This values are compared with the actual motor torque fed from the hall sensors. The reference current is generated by the error signals produced by the reference torque and the measured actual torque [14, 15]. The reference current and the measured current generated error signals is fed to the hysteresis current controller. The gate pulses to a VSI switches to turn ON or OFF is produced by the hysteresis current controller. The DC link capacitor acts as the source to a voltage source converter. All the feedback to generate the error signal are sensed by the hall sensors. Speed control by the current control method yields better results [16].

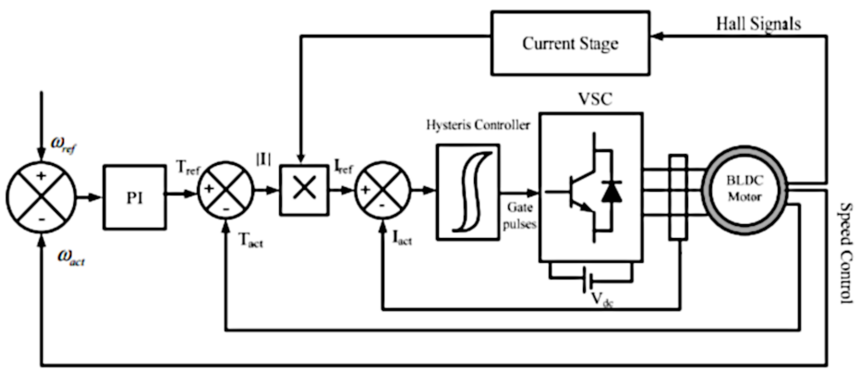

Figure 2. Schematic diagram of speed control of BLDC motor

2.2. Mathematical modelling of the BLDC motor

Consider a cylindrical rotor and stator as having three phase windings, namely, a, b, and c. The rotor is of permanent magnets with a uniform air gap, while the stator has three phases, which are star-connected. The motor is not saturated as it is operated within the rated current. The dynamic equations of phase a, phase b, and phase c are:

$$V_{an} = R_S + L\frac{di_a}{dt} + M\frac{di_b}{dt} + M\frac{di_c}{dt} + e_a \tag{1}$$

$$V_{bn} = R_S + L\frac{di_b}{dt} + M\frac{di_c}{dt} + M\frac{di_a}{dt} + e_b \quad (2)$$

$$V_{cn} = R_S + L\frac{di_c}{dt} + M\frac{di_a}{dt} + M\frac{di_b}{dt} + e_c \quad (3)$$

Where, R is the resistance of the armature, L is the self-inductance of the armature, M is the mutual inductance of the armature, V_{an}, V_{bn}, and V_{cn} is the voltage of the terminals, and i_a, i_b, and i_c is the input current of the motor.

$$\begin{bmatrix} V_{an} \\ V_{bn} \\ V_{cn} \end{bmatrix} = \begin{bmatrix} R_S & 0 & 0 \\ 0 & R_S & 0 \\ 0 & 0 & R_S \end{bmatrix} \begin{bmatrix} i_a \\ i_b \\ i_c \end{bmatrix} + \begin{bmatrix} L & M & M \\ M & L & M \\ M & M & L \end{bmatrix} \begin{bmatrix} i_a \\ i_b \\ i_c \end{bmatrix} + \begin{bmatrix} e_a \\ e_b \\ e_c \end{bmatrix} \quad (4)$$

In the BLDC motor, the function of a rotor position is related to the back emf. Each phase of the back emf has 120^0 phase angle differences. Therefore, the equations for each phase are as follows:

$$e_a = K_a f_a(\theta)\omega_r \quad (5)$$

$$e_b = K_b f_b(\theta + \frac{2\pi}{3})\omega_r \quad (6)$$

$$e_c = K_c f_c(\theta - \frac{2\pi}{3})\omega_r \quad (7)$$

$$\begin{bmatrix} V_{an} \\ V_{bn} \\ V_{cn} \end{bmatrix} = \begin{bmatrix} R_s & 0 & 0 \\ 0 & R_s & 0 \\ 0 & 0 & R_s \end{bmatrix} \begin{bmatrix} i_a \\ i_b \\ i_c \end{bmatrix} + L_s \begin{bmatrix} \frac{di_a}{dt} \\ \frac{di_b}{dt} \\ \frac{di_c}{dt} \end{bmatrix} + \begin{bmatrix} e_a \\ e_b \\ e_c \end{bmatrix} \quad (8)$$

The total torque was as follows:

$$e_a = K_a \omega_r \quad (9)$$

$$P_m = e_a i_a + e_b i_b + e_c i_c \quad (10)$$

$$T_e = \frac{P_m}{\omega_{rm}} = \frac{(e_a i_a + e_b i_b + e_c i_c)}{\omega_r}\frac{P}{2} \quad (11)$$

$$T_e = \frac{P(K_a i_a + K_b i_b + K_c i_c)}{2} \quad (12)$$

Mechanical part

$$T_e - T_L = J\frac{d\omega_{rm}}{dt} + B\omega_{rm} \quad (13)$$

$$\frac{d\omega_{rm}}{dt} = \frac{P}{2J}(T_e - T_L - \frac{2B}{P}\omega_r) \quad (14)$$

Where, T_e is the electromagnetic torque, B is the flux density, T_L is the load torque, and J is the current density [17].

2.3. System design

For the desired operation of the mixer grinder, suitable specifications and design of the PV array, Buck converter, and the BLDC mixer grinder play an important role. A 4-pole BLDC motor with 10000 rpm and 200W is selected. The PV array, Buck converter, and mixer grinder are selected so that the function of a system is not disturbed under any climatic conditions.

2.3.1. PV array and maximum power point tracking (MPPT)

A PV array with peak power of 300W was designed for a 200W mixer grinder in order to compensate the motor and converter losses. Table 1 shows the design of the PV array, and the MPPT technique used is the Perturb and Observer algorithm as shown in Figure 3. This algorithm uses less measuring parameters and a simple feedback. In this method, the voltage of a module is periodically given a perturbation, and the consistent power output is compared with the prior perturbing cycle. Due to the perturbation, if the power increases, then perturbation is continued in the same direction. After a peak power is reached, the power at the MPP is zero and the next instant decreases, then perturbation reverses. When steady state condition is reached, the algorithm oscillates around a peak power point. In order to sustain small power variations, the perturbation size maintained very small. The method is advanced so that it sets a reference voltage of a module corresponding to the peak voltage of a module. A PI controller acts to transfer an operating point of the module to that particular voltage level. It is seen that some power loss occurs due to this perturbation. The MPPT algorithm operates on the derivative of an output power (P) with respect to the panel voltage (V), which is equal to zero at MPPT [18].

Table 1. Design of PV array

PV module (HB-12100)	
N_s	36
V_o	21V
I_o	7.1A
V_m	17V
I_m	6A
V_{oc}	63V
I_{sc}	7.1A
Modules in series	3
Modules in parallel	1
Peak Power	300W

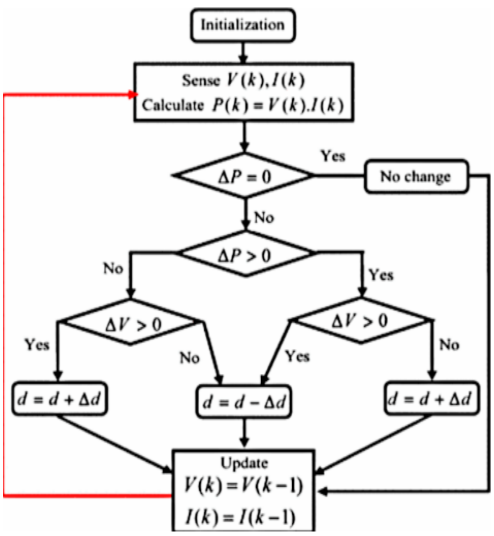

Figure 3. Flowchart of the perturb and observer algorithm

2.3.2. Buck converter

The Buck converter is the DC-DC converter, which steps downs the voltage from its high input voltage. Figure 4 represents the circuit of the Buck converter. Table 2 shows the specifications of the buck converter.

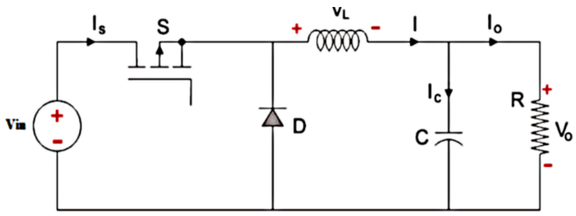

Figure 4. Circuit of the buck converter

Table 2. Specifications of the buck converter

Input voltage (V_{in})	51.6V
Output voltage(V_o)	48V
Switching frequency(f_{sw})	500kHz
Inductor current ripple (I_{ripple})	30%
Output voltage ripple(V_{ripple})	10mV

To calculate the value of the inductor:

$$V = L * \frac{\Delta I}{\Delta T} \tag{15}$$

$$L = (V_{in} - V_{out}) * \frac{\frac{D}{f_{sw}}}{I_{ripple}} \tag{16}$$

L=11.16µH

To calculate the value of the capacitor:

$$C_{\min} = \frac{(\Delta I * \Delta T)}{(\Delta V - (\Delta I * ESR))} \tag{17}$$

Given, ESR (Effective series resistance) is 0.03Ω, $\Delta I = 0.6A$, and $\Delta T = 0.8\mu$ sec:

C_{min}=15µF

$$C = \frac{\Delta T}{((\frac{V_{ripple}}{I_{ripple}}) - ESR)} = 470\mu F \tag{18}$$

Table 3 shows the switching states of the VSI. The three hall sensors are used to produce gate signals to the VSI by electronic commutations. Electronic commutations refer to a commutation of the currents flowing through the windings of the BLDC motor in predefined sequences by the decoder such that direct current symmetrically is drawn from a DC bus of the VSI for 120° and placed in a phase with the back emf. The VSI is operated through the fundamental frequency switching pulses for reducing switching losses. Table 4 represents the specifications of the BLDC motor.

Table 3. Switching states of VSI [11]

Rotor position θ	Hall signal			Switching state					
	H_3	H_2	H_1	S_1	S_2	S_3	S_4	S_5	S_6
NA	0	0	0	0	0	0	0	0	0
0-60	1	0	1	1	0	0	1	0	0
60-120	0	0	1	1	0	0	0	0	1
120-180	0	1	1	0	0	1	0	0	1
180-240	0	1	0	0	1	1	0	0	0
240-300	1	1	0	0	1	0	0	1	0
300-360	1	0	0	0	0	0	1	1	0
NA	1	1	1	0	0	0	0	0	0

Table 4. Specification of BLDC motor

Rated Power	200W
Input Voltage	48V
Speed	10000RPM
Stator Resistance(R_s)	0.6ohms
Stator Inductance (L_s)	0.06mH
Number of Poles (P)	4
Friction Coefficient (B)	0.0682e-3
Inertial Coefficient (J)	21.5e-3 J/kgm^2

3. RESULTS AND ANALYSIS

The proposed solar based current controlled BLDC mixer grinder was simulated in the MATLAB software. The solar irradiance was varied from 500W/m^2-1000W/m^2, and power output of the PV array is depicted in Figure 5. From Figure 5, it can be concluded that when the solar irradiance is 1000W/m^2, maximum output power is obtained from the PV panel. Figure 6a and 6b represents the output voltage and output power from the Buck converter when the solar irradiance is 1000W/m^2.

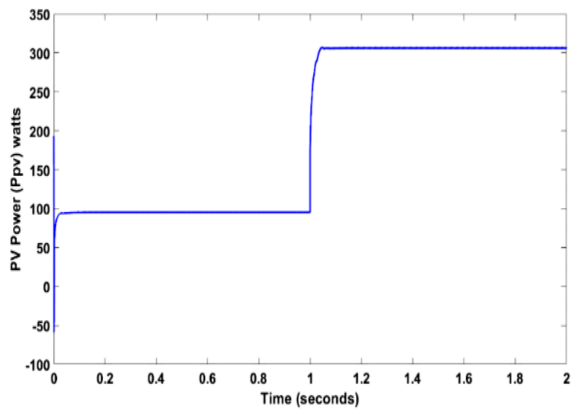

Figure 5. Power output from the PV panel

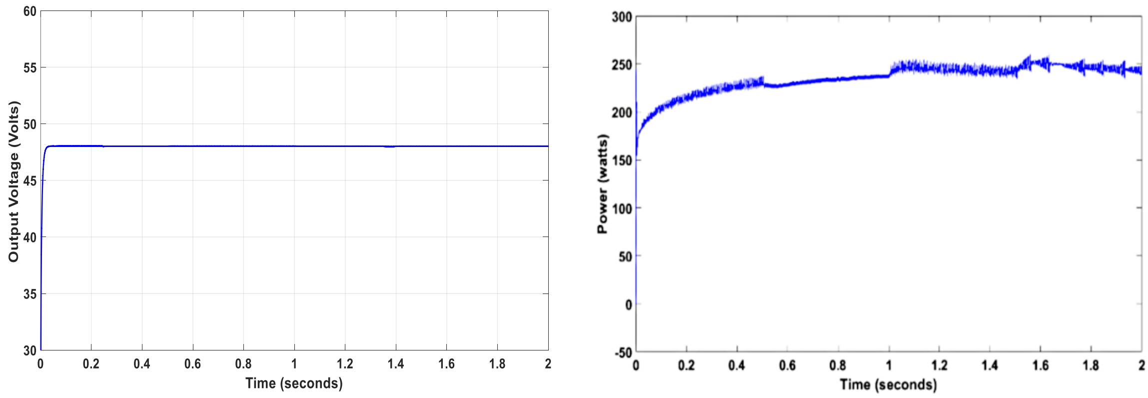

(a) (b)

Figure 6. Output voltage and power from the buck converter

From the PI controller, the speed was regulated as depicted in Figure 7. The reference speeds and measured speeds is summed, and an error signals generated is given to a PI controller to nullify the error signal [19]. Figure 8 represents the measured torque of the BLDC motor. Initially, when the back emf is zero, the torque is high, and as the speed increases, the torque decreases [20-21]. Figure 9 illustrates the phase currents of a BLDC motor. As the load increases, the motor draws more current [22-23]. When the speed is increased, the current drawn increases [24, 25].

The Philips HL 1643/04 model was used for the experimental demonstration as depicted in Figure 10. The specifications of this model are 600W, 230V AC, and speed of 18000 rpm. Flux 435 series II power quality and energy analyzer was used for taking the readings as shown in Figure 10. Table 5 shows the comparison of an existing mixer grinder and the simulated the proposed 48V BLDC system. If the crest factor is around 1.41, then there is an absence of distortion, and if the crest factor is above 1.8, then the amount of distortion is very high [26].

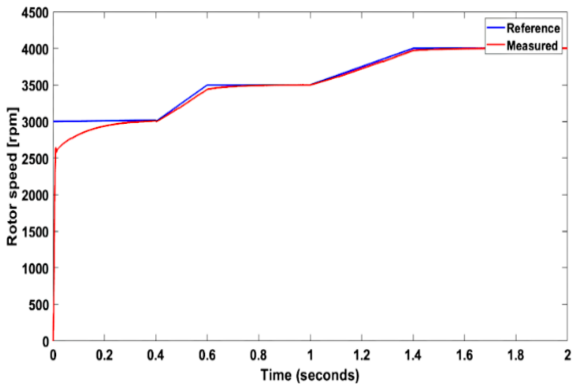

Figure 7. Reference and measured speed from the 200W BLDC motor

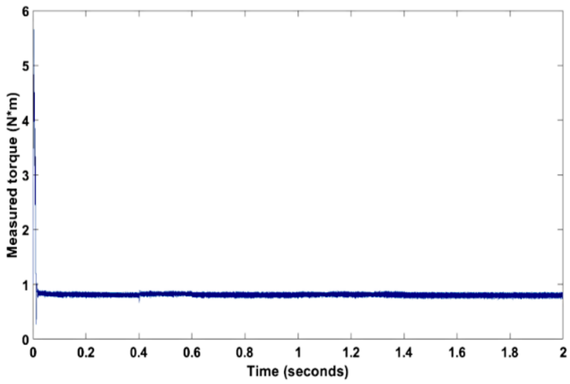

Figure 8. Measured torque of the BLDC motor

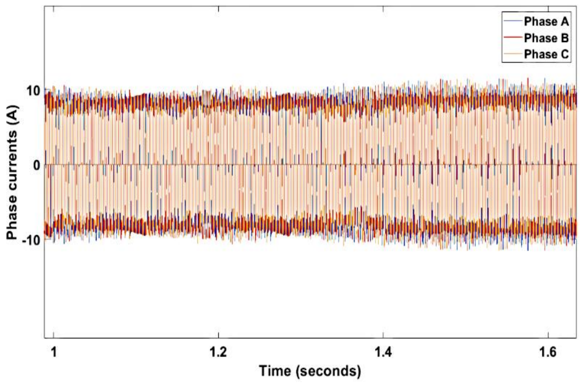

Figure 9. Phase currents of the BLDC motor

Figure 10. Experimental demonstration of existing mixer grinder

Table 5. Comparison of the experimental existing mixer grinder and simulated proposed 48V BLDC system

	Experimental existing mixer grinder (600W) No load	Simulated proposed mixer grinder (200W) No load	Experimental existing mixer grinder (600W) With load	Simulated proposed mixer grinder (200W) With load
Amount of distortion (Crest factor)	Cf=2.39	Cf=1.41	Cf=2.05	Cf=1.39
Total Harmonic distortion	Voltage=5% Current=20.2%	Voltage=3.35% Current=3.25%	Voltage=4.8% Current=15.3%	Voltage=3.15% Current=3.05%
The efficiency of the system	51.03%	81.25%	49.32%	79.85%

4. CONCLUSION

As per the specification data, the proposed 48V BLDC mixer grinder was simulated in the Matlab/Simulink. The proposed closed loop current controller of the BLDC system was discussed. The torque, variable speed, and the stator currents characteristics were also discussed. A comparative analysis of the efficiency and the harmonic distortion of the experimental existing universal motor and the simulated proposed BLDC motor system was determined. Due to the absence of friction of the brushes, the efficiency of the 48V BLDC motor was higher than that of the mixer grinder operated in the universal motor. The crest factor and the total harmonic distortion was higher in the existing universal motor compared with the proposed system.

ACKNOWLEDGEMENTS

I would like to thank my guide (Dr. R. Shivarudra Swamy) for his guidance in this research paper. I thank my HOD for his support, and my college (Manipal Institute of Technology, Manipal), which provided the expertise that greatly assisted the research. I would like to thank Mr. Jayaraj for helping in the experimental demonstration of the mixer grinder.

REFERENCES

[1] Vithayasrichareon P, "Valuing large-scale solar photovoltaics in future electricity generation portfolios and its implications for energy and climate policies," *IET Renewable Power Generation*, vol. 10, pp. 78-87, 2016.

[2] Hirth L., "Market value of solar power: is photovoltaics cost-competitive?," *IET Renewable Power Generation*, vol. 9, pp. 38-45, 2014.

[3] Hwang, Li P.L, Liu T, *et al*., "Design and analysis of a brushless DC motor for applications in robotics," *IET Electric Power Appl.*, vol. 6, pp. 385-389, 2012.

[4] Cheng M.Y, Chi W.C, Chen C.H, "Position-sensorless method for electric braking commutation of brushless DC machines," *IET Electric Power Appl*., vol. 7, pp. 701-713, 2013.

[5] Bist V, Singh B, "A unity power factor bridgeless isolated cuk converter-fed brushless DC motor drive," *IEEE Trans. on Indus. Electronics*, vol. 62, pp. 4118-4129, 2015.

[6] Shakouhi S.M, Mohamadian, Afjei E, "Torque ripple minimization control method for a four phase brushless DC motor with non-ideal back-electromotive force," *IET Electric Power Appl*., vol. 7, pp. 360-368, 2013.

[7] Xia C, Chen W, Xiao Y, *et al*., "Three effective vectors-based current control scheme for four-switch three-phase trapezoidal brushless DC motor," *IET Electric Power Appl*., vol. 7, pp. 565-574, 2013.

[8] Kumar R, Singh B, "BLDC motor driven solar PV array fed water pumping system employing zeta converter," *IEEE Transactions on Industrial Appl*., vol. 52, pp. 2315-2322, 2016.

[9] Huang H.H, Chen H.C, "Design of buck-type current source inverter fed brushless DC motor drive and its application to position sensorless control with square-wave current," *IET Electric Power Appl*., vol. 7, pp. 416-426, 2013.

[10] Kumar R, Singh B, "Simple brushless DC motor drive for solar photovoltaic array fed water pumping system," *IET Power Electronics*, vol. 9, pp. 1486-1495, 2016.

[11] Xia CL, *Permanent magnet brushless DC motor drives and controls*, John Wiley & Sons, 2012.

[12] Kumar Rajan, Bhim Singh, "Solar PV powered BLDC motor drive for water pumping using cuk converter," *IET Electric Power Applications*, vol. 11, pp. 223-232, 2017.

[13] Mozaffari Niapour, Danyali S, Sharifian, *et al.*, "Brushless DC motor drives supplied by PV power system based on Z-source inverter and FL-IC MPPT controller," *Energy Conversion Management*, vol. 52, pp. 3045-3059, 2011.

[14] Hosseini, Nejabatkhah F, Mozafari Niapoor, *et al*., "Supplying a brushless dc motor by z-source PV power inverter with FL-IC MPPT," *2010 International Conf. on Green Circuit and System*, Shanghai, pp. 485-490, 2010

[15] Elgendy, Atkinson, Zahawi B, "Experimental investigation of the incremental conductance maximum power point tracking algorithm at high perturbation rates," *IET Renewable Power Gen*., vol. 10, pp. 133-139, 2016.

[16] Sarala P, Kodad, Sarvesh, "Analysis of closed-loop current controlled BLDC motor drive," *In 2016 International Conf. on Electronics, Electrical and Optimization Techniques, IEEE*, pp. 1464-1468, 2016.

[17] Ghasemi, Mohammadian Forushani H, Parniani M, "Partial shading detection and smooth maximum power point tracking of PV arrays under PSC," *IEEE Trans. on Power Electronics*, vol. 31, pp. 6281-6292, 2015.

[18] Sundareswaran K, Vigneshkumar V, Palani S, "Development of a hybrid genetic algorithm/perturb and observe algorithm for maximum power point tracking in photovoltaic systems under non-uniform insolation," *IET Renewable Power Gen*., vol. 9, pp. 756-765, 2016.

[19] Deekshitha S. Nayak, Swamy Shivarudra R, "Loss and efficiency analysis of universal motor used in mixer grinder by mathematical modelling," *In 2018 IEEE International Conf. on Automatic Control and Intelligent Systems*, pp. 105-110, 2018.

[20] K.D. Lee, J. S. Park, "Online advanced angle adjustment method for sinusoidal BLDC motors with misaligned hall sensors," *IEEE Transactions on Power Electronics*, vol. 32, pp. 8246-8254, 2017.

[21] S. Zheng, H. Li, H. Ren, "Self-correction of commutation point for high-speed sensorless BLDC motor with low inductance and non-ideal back EMF," *IEEE Trans. on Power Electronics*, vol. 32, pp. 643-652, 2017.

[22] S. Chen, G. Liu, L. Zhu, "Sensorless control strategy of a 315 kW high speed BLDC motor based on a speed-independent flux linkage function," *IEEE Trans. on Industrial Elect*., vol. 64, pp. 8607-8617, 2017.

[23] M. S. Ahmad, A. A. M. Nurul, F. Maher and I. Dahaman, "Improved torque in PM brushless motors with minimum difference in lot number and pole number," *International Journal Power and Energy Conversion*, vol. 3, pp. 206- 219, 2012.

[24] Z. Q. Zhu, H. David Howe and C. C. Chan, "Improved analytical model for predicting the magnetic field distribution in brushless permanent-magnet machines," *IEEE Transactions on Magnetics*, vol. 38, pp. 229-238, 2002.

[25] Nayagam V Senthil and L. Premalatha, "Green energy based coupled inductor interleaved converter with MPPT technique for BLDC application," *International Journal of Power Electronics and Drive Systems*, vol. 9, pp. 1725-1732, 2018.

[26] Ahmed Akram H, B. Abd El Samie and Ayman M Ali, "Comparison between fuzzy logic and PI control for the speed of BLDC motor," *International Journal of Power Electronics and Drive Systems*, vol. 9, pp. 1116-1123, 2018.

BIOGRAPHIES OF AUTHORS

Deekshitha S. Nayak, Research Scholar in the Department of Electrical and Electronics Engineering in Manipal Institute of Technology, Manipal.Completed B. E (Electrical and Electronics) degree at YIT Moodbidri in the year 2014 and M. Tech (Electronics) degree at Canara Engineering College in the year 2016.The area of interest are Renewable Energy, Power Electronics, Motor and Drives.

Dr. R. Shivarudraswamy, Working at Manipal Institute of Technology, Manipal, in the Department of Electrical & Electronics as an Associate Professor from last 15 Years, before worked in the Industry as an Electrical Maintenance Engineer about 3 and half years. Completed B. E (Electrical) degree at SIT Tumkur in year 1994 & M. Tech degree at Malnad College of Engineering in the year 2002 & completed Ph. D degree at NITK Surathkal, Karnataka in the year 2013. The area of research Interest are Distributed Generators and Energy conservation and Management. Published many papers in the National & International Conferences & Journals.